united nations educational, scientific and cultural organization

international atomic energy agency

the
abdus salam
international centre for theoretical physics

Course on "Inverse Methods in Atmospheric Science"
1 - 12 October 2001

301/1332-19

"DOAS Retrievals"

M. VAN ROOZENDAEL
Belgian Institute for Space Aeronomy
Brussels

Please note: These are preliminary notes intended for internal distribution only.

DOAS retrievals

Michel Van Roozendael
Belgian Institute for Space Aeronomy

Outline

- What is DOAS ? Principle and basic equations
- Optimum instrumental design
- DOAS applications
  - Long-path (active DOAS)
  - Balloon-borne solar occultation DOAS
  - Zenith-sky DOAS
  - DOAS from satellite
- Future of DOAS

What is DOAS ?

- **DOAS** = **D**ifferential **O**ptical **A**bsorption **S**pectroscopy
- Technique of remote sensing allowing the determination of the abundance of atmospheric trace species by use of their structured absorption bands in the UV and visible spectral regions
- **Absorption spectroscopy**
  - Beer-Lambert law :
  - Absorption spectroscopy:

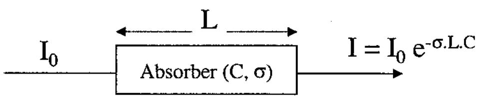

$$C = -\frac{1}{\sigma.L}.\ln\left(\frac{I}{I_0}\right)$$

  - Problems for atmospheric applications:
    - Usually I_0 cannot be easily determined
    - Several terms (incl. molecular absorption and scattering) contribute to the total attenuation at one wavelength (spectral interference)

Differential absorption technique : early days

- Atmospheric molecular species show structured absorption bands in the UV and visible regions, e.g. O_3 in the Huggins bands

→ Basic idea pioneered by Dobson in the 1930s in designing the famous Dobson total ozone spectrophotometer : the total atmospheric abundance of O_3 can be derived from a measure of the relative intensities of the solar light at 2 (or more) UV wavelengths.

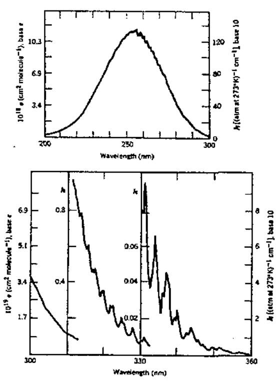

Fig. 1 UV spectrum of ozone.[14]

Gordon Dobson

The Dobson spectrophotometer

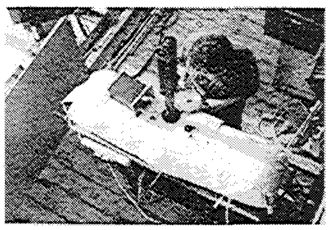

Dobson equation:

Rayleigh scattering term ↓   Aerosol term ↓

$$I = I_0 \exp\{-[\alpha.X.\mu + \beta.M + \delta.A]\}$$

$$I' = I'_0 \exp\{-[\alpha.'X.\mu + \beta.'M + \delta'.A]\}$$

↓ Ratioing, taking logarithm and regrouping terms:

$$X = \frac{N - (\beta - \beta').M - (\delta - \delta').A}{(\alpha - \alpha').\mu}$$

N factors: $N = \ln(\frac{I}{I'_0}) - \ln(\frac{I}{I'})$

where:
α = O_3 absorption coefficient
X = O_3 total column
μ = geometric airmass factor

The O_3 absorption is the main factor affecting the relative intensities at the pair of wavelengths !

Modern DOAS

- Extension of the differential absorption method to other trace species than O_3 triggered by the development in the 1980s of low-noise multichannel array detectors → full spectral information available with high S/N ratios (>10^4)
- **Principle of modern (spectral) DOAS:**

$$I^\lambda = I_0^\lambda \exp\left(-\tau_{Rayleigh} - \tau_{Mie} - \tau_a\right)$$

↓

$$\ln I^\lambda = \underbrace{\ln I_0^\lambda - \tau_{Rayleigh} - \tau_{Mie}}_{\text{broadband}} \underbrace{- \tau_a}_{\text{structured}}$$

broadband ↓ can be approximated by a smooth function of λ (e.g. polynomial)

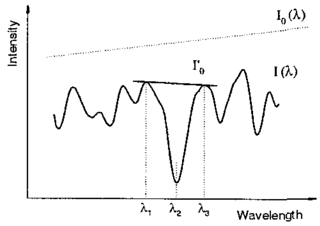

DOAS principle (cont.)

- **Differential cross-sections**
  - Although not absolutely needed, it is a usual practice to use differential cross-sections obtained by separating the low-frequency part from the high frequency part of the cross-sections:

$$\sigma(\lambda) = \sigma'(\lambda) + \sigma_{broadband}(\lambda)$$

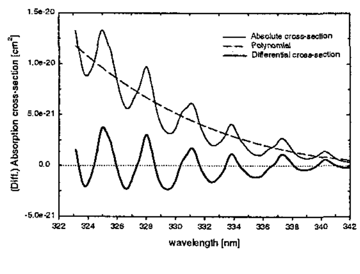

→ DOAS basic equation:

$$\ln I^\lambda = \ln I_0^\lambda - P(\lambda) - \sum_i \sigma'_i . N_i$$

where: $P(\lambda)$ = polynomial
σ_i = differential cross-section of species i
N_i = slant column of species i

DOAS retrieval in practice

- Actual DOAS retrievals are often complicated by the need to account for additional effects which might be application-specific (some of them will be further developed later in the talk)
- One common and very usual problem found in practice is the need to account for inaccuracies or instabilities in the wavelength registration of both laboratory cross-section data and measured spectra, which leads to a slight modification of the DOAS equation:

$$\ln I(a+b\lambda) = \ln I_0^{\lambda} - P(\lambda) - \sum_i \sigma'_i . N_i$$

where a, b are **shift and stretch parameters** simultaneously fitted, together with N_i and polynomial coefficients, in a **non-linear least-squares process**. Similar shift and stretch parameters may have to be considered for the σ_i' as well.

Differential absorption cross-sections

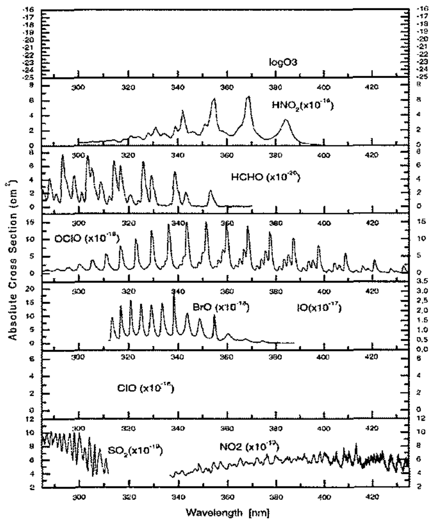

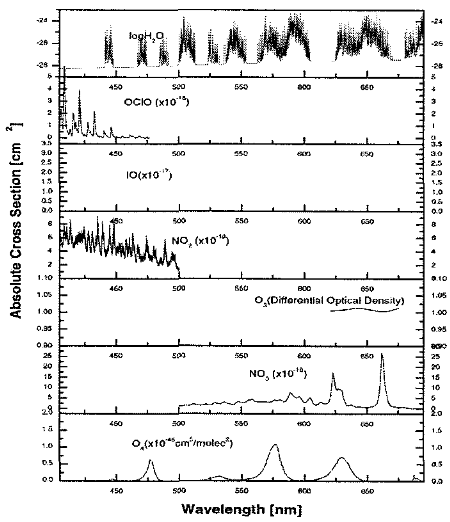

Optimum instrumental design (1)

- **Optimum resolution** → trade-off between resolution and sensitivity, optimum resolution determined by the width of the molecular absorption structures (typically 0.2 to several nm depending on species)
- **Spectrometer design** : grating versus Fourier Transform spectrometers

  FTS → high resolution, accurate wavelength registration but low sensitivity and high cost

  Grating spectrometers → low resolution, wavelength registration unstable, but high light throughput, simplicity and (relatively) low costs → optimal choice for most DOAS applications
- **Detectors** – requirements: low noise, high sensitivity

  → Cooled diode-array detectors (high sensitivity, fast readout)

  → new generation of CCD (back-illuminated, UV-enhanced sensitivity - slow readout, but 2D imaging capability opens new applications)

Optimum instrumental design (2)

- **Polarisation response** of grating spectrometers
  - Potential source of artefact for applications using polarised light sources (e.g. the zenith sky light). Optimised DOAS instruments use fiber optic bundles to depolarise incoming light, or select one constant direction of polarisation
- **Optimum wavelength sampling** → trade-off between sampling and spectral coverage (array detectors usually limited to 1000-2000 pixels max.).

! The slit function must be oversampled to minimise interpolation errors → the optimum is approx. 6 pixels/FWHM

(Roscoe et al., *App.Optics* 35,427,1996)

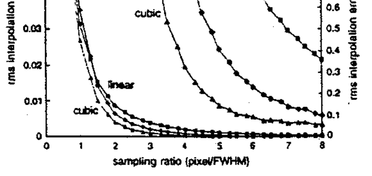

DOAS remote-sensing applications

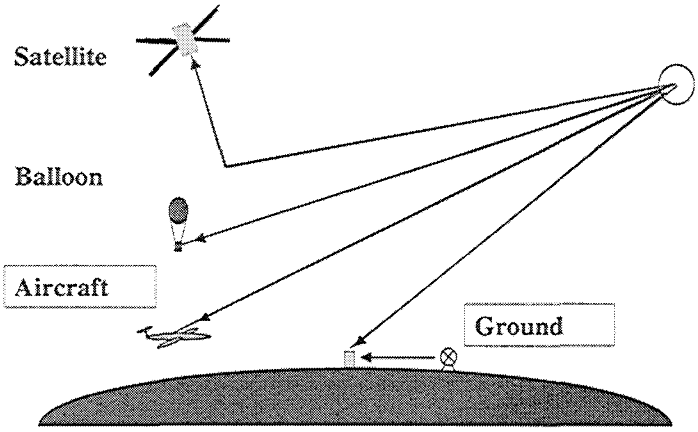

Long-path DOAS

- **Applications** : air pollution monitoring and process studies
- **Light sources** → <u>requirements</u>: minimum spectral variations, brightness
  - Incandescent lamps or arc lamps (e.g. Xenon arc lamps)
  - Laser (DOAS measurement of OH)
- **Difficulties:**
  - Unwanted spectral structures in light source spectrum (e.g. atomic lines)
  - Stray-light rejection – important because stray-light reduces measured optical densities !
  - Spectral interferences → fitting windows must be choosen to minimise the correlation between cross sections of species absorbing in the same interval
  - <u>**Variations of the angular distribution of the light source intensity**</u> → produces unwanted residuals due to angular dependence of PDA response. Can be minimised by the use of a quartz-fiber mode coupler.

Illumination of spectrograph-detector system

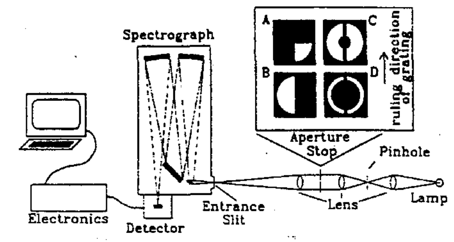

Fig. 1. Experimental setup to investigate the dependence of the spectrograph–detector system on the illumination. The aperture stops *A, B, C,* and *D* are inserted into the collimated light beam, which is produced by two lenses and a 200-μm pinhole. The light is focused on the entrance slit of the spectrograph by another lens.

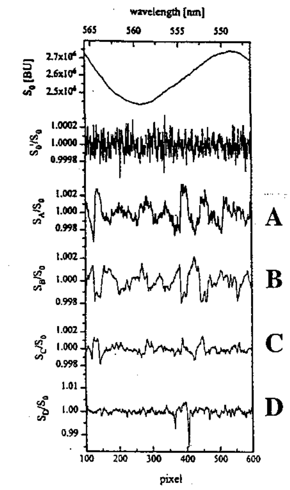

(Stutz et al., *App.Optics* 36, 1105, 1997)

The fiber mode mixer solution

Mode mixer setup

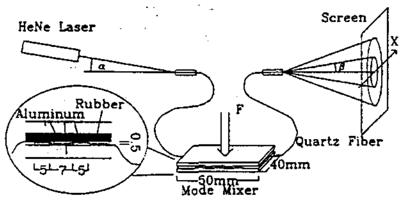

Fig. 5. Experimental setup to investigate mode coupling in a multimode quartz fiber. The light beam of a helium–neon laser is fed into the fiber at an angle α. The fiber is placed between two plates with a step profile. A sheet of rubber is placed between the top aluminum plate and the profile to protect the fiber. The plates can be pressed together with a force *F* to introduce microbending to the fiber. The light intensity leaving the fiber is measured with a photoresistor on a screen at a 15-cm distance from the fiber end along the X axis.

(Stutz et al., *App.Optics* 36, 1105, 1997)

→ **Improvement of residuals by one order of magnitude !**

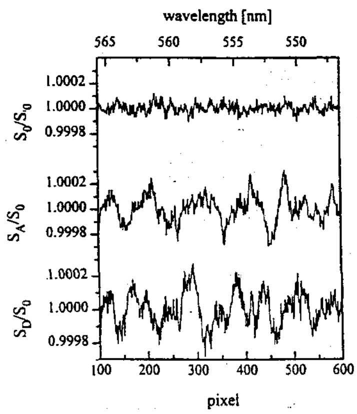

Balloon-borne solar occultation DOAS

- Vertical profiles can be derived (onion peeling method) from measurements during ascent and occultation
- **Relevant molecules** : NO_2, O_3, OClO, BrO, IO (?), HCHO, H_2O, O_4
- **Application**: stratospheric ozone chemistry – processes, model verifications, satellite validation...

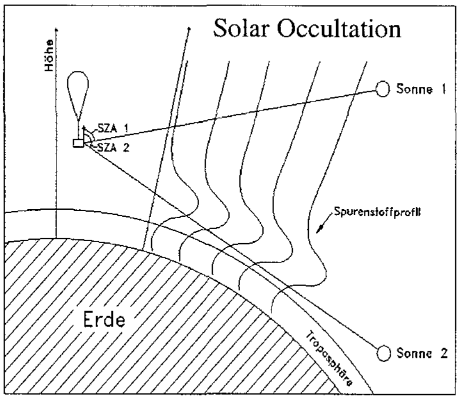

Launch of LPMA/DOAS balloon in Leon (Spain), March 1998

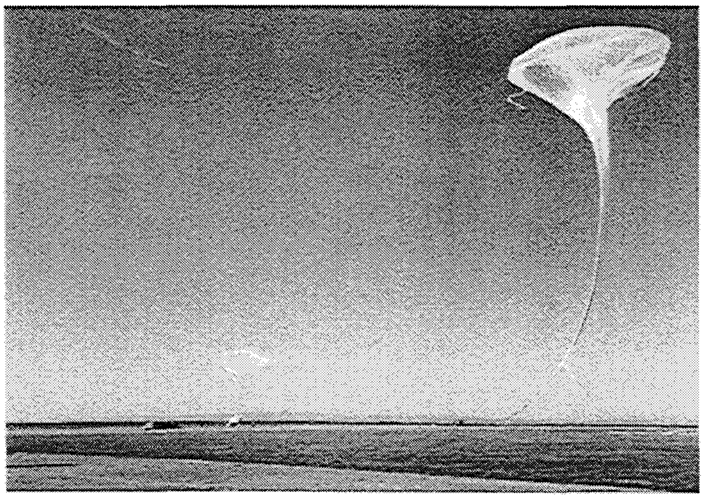

DOAS using solar light as a source

- Solar spectrum highly structured in the UV and visible regions
- **Advantage:** solar structures can be used as internal wavelength calibration
- **Difficulties:**
  - **Solar I_0 effect :**
    - laboratory cross sections are usually not measured with the field instrument using the sun as source, hence they must be filtered to match the instrument resolution.

Problem:
$$F \otimes \{I_0 e^{-\tau}\} \neq \{F \otimes I_0\}.e^{-F \otimes \tau} \quad (F = \text{Instrument slit function})$$

Solution:
$$\sigma_{corrected} = \frac{-1}{X} \ln \left[\frac{F \otimes I_0 \exp(-\sigma.X)}{F \otimes I_0} \right] \quad \leftarrow \textbf{Solar } I_0 \textbf{ correction}$$

  - **Residual amount in the reference spectrum**
    - **The control spectrum (I_0) is not measured outside the atmosphere → usually it contains a residual atmospheric absorption which must be estimated (Langley plot technique) and added to the measured slant column.**

Wavelength calibration using solar lines

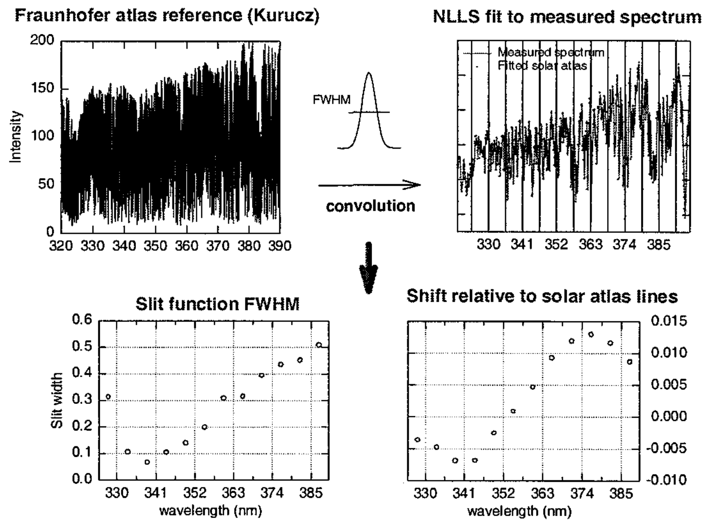

Occultation Geometry

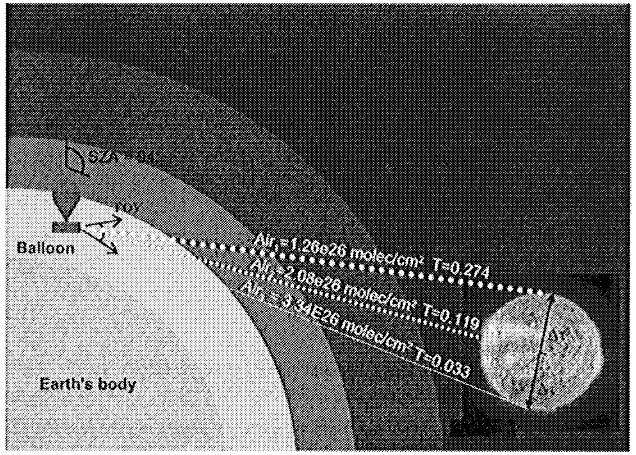

Hartmut Boesch

Institut für Umweltphysik
University of Heidelberg

Solar Center – Limb Darkening (CLD)

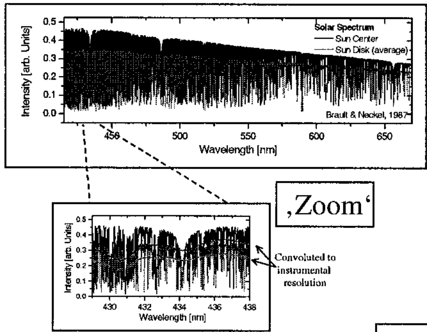

Assumption :

$I_0 \rightarrow I_0 + a\,(I_0 - I_c)$

Fitting Procedure:

$\ln\,(I_0(1+a(I_0 - I_c)/I_0))$

$\approx \ln I_0 + a\,((I_0 - I_c)/I_0))$

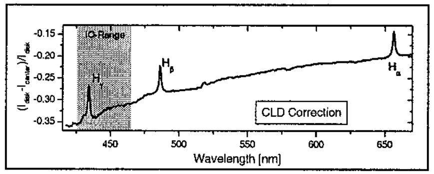

Hartmut Boesch

Institut für Umweltphysik
University of Heidelberg

IO Evaluation (1)

[naive approach]

Kiruna, Northern Sweden
Feb. 10, 1999, SZA = 94.5°

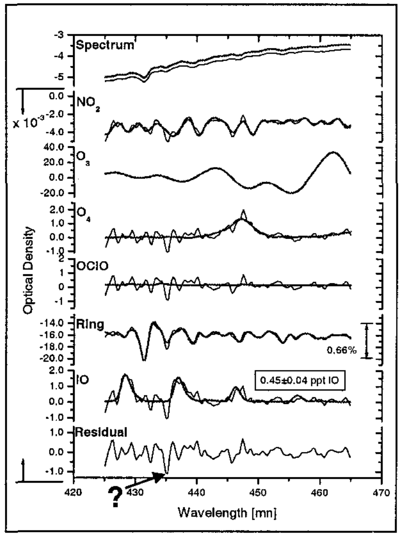

Hartmut Boesch

Institut für Umweltphysik
University of Heidelberg

Solar Center - Limb Darkening

- Emission at distance r (or with angle θ) comes from higher and colder layers
- λ-Dependent intensity decrease towards limb
- Effect occurs also for absorption lines, but dependence on r is different
- Optical densities of Fraunhofer lines are changing: OD = OD (r)

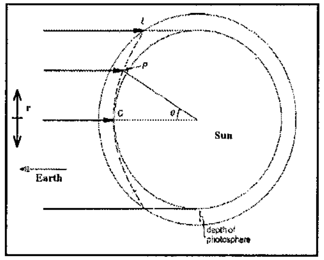

Hartmut Boesch

Institut für Umweltphysik
University of Heidelberg

IO Evaluation (3)

[advanced approach]

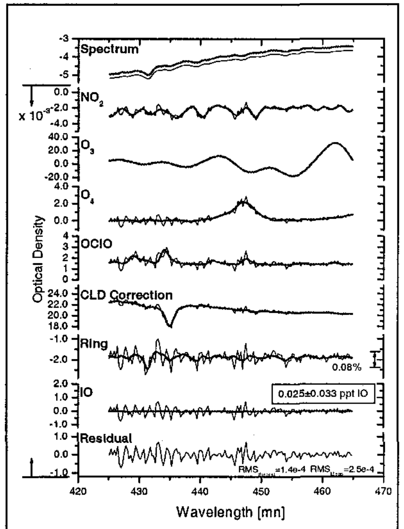

Kiruna, Northern Sweden
Feb. 10, 1999, SZA = 94.5°

Hartmut Boesch
Institut für Umweltphysik
University of Heidelberg

Zenith-sky DOAS

- Total columns of stratospheric species can be retrieved from measurements of the zenith sky light at twilight – Operational advantages : easy to operate, weakly affected by clouds
- **Application**: monitoring of stratospheric trace species – NDSC (Network for the Detection of Stratospheric Change)
- **Relevant molecules**: NO_2, O_3, BrO, OClO, IO, …, HCHO, H_2O, O_4, SO_2

Zenith-sky geometry

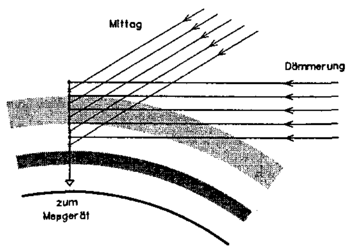

Abbildung 3.1: Beobachtungsgeometrie für Zenitmessungen.

Zenith sky DOAS retrieval

- **The optically thin atmosphere approximation**
  - The effective absorption seen in zenith-sky radiances corresponds to a complex combination of photons having travelled through a scattering/absorbing atmosphere. Stricly speaking the DOAS method is only applicable if the effective photon path-length through the absorbing layer of interest doesn't vary too much with the wavelength (true for an optically thin atmosphere).

→ **Zenith-sky DOAS equation:**

$$\ln I^{\lambda} = \ln I_0^{\lambda} - P(\lambda) - \sum_i \sigma'_i(\lambda).V_i.AMF_i$$

where V_i = vertical column

AMF_i = single wavelength air mass factor

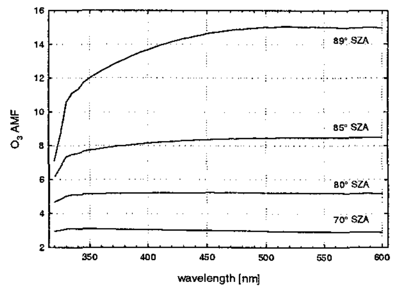

AMFs and vertical profiling capabilities

- AMF calculation requires radiative transfer modeling → $AMF = \frac{Slant\ column}{Vertical\ column}$
- Weak dependence on vertical profile shape (stratosphere) up to 90° SZA

- Above 90° SZA, the dependence of the AMFs on the altitude of the absorber can be used to derive low resolution (5 km at best) vertical distributions. Method demonstrated for NO_2.

(Preston et al., JGR 102, 19089, 1997)

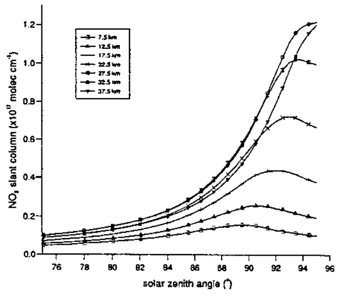

Figure 3.1: *The variation of NO_2 slant column values with SZA for Gaussian (FWHM = 5 km) NO_2 profiles with the peak mixing ratio at different altitudes (see legend). Chemistry is included and a 2-D slant column calculation (see Chapter 4) is used.*

NO_2 vertical profiling

Weighting functions

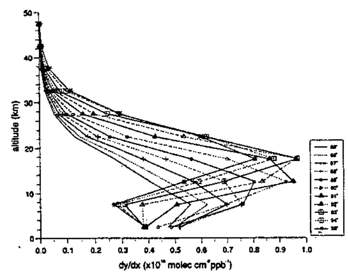

Figure 3.3: *A series of weighting functions based on column model output for Cambridge (52°N) in July. Each weighting function corresponds to a different measurement SZA (see legend).*

Averaging kernels

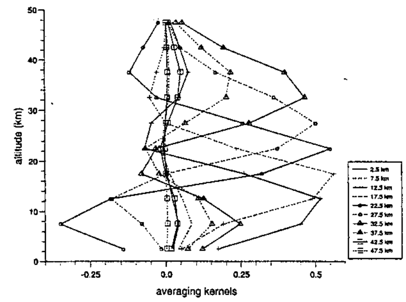

Figure 5.2: *Averaging kernels calculated using a typical NO_2 vertical profile for Cambridge (52°N) in July. Each averaging kernel corresponds to a different profile altitude (see legend).*

Ring effect

- Rotational Raman scattering by molecular N_2 and O_2 responsible of the so-called Ring effect (inelastic scattering process)
- Very significant effect – can be measured or modelled

Raman cross-sections of N_2 and O_2

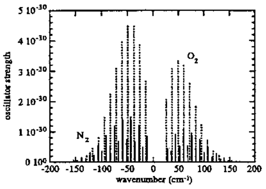

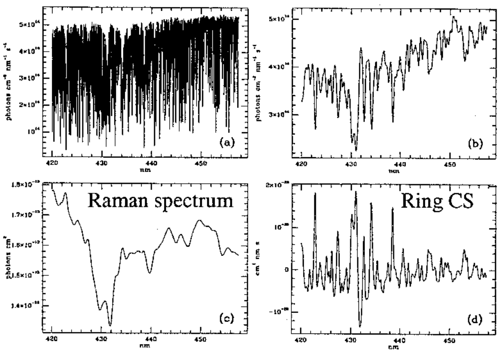

(Chance and Spurr, *App.Optics, 36*, 5224,1997)

Photochemical effects

- Interpretation of zenith-sky measurements of photochemically active species like BrO and OClO complicated by the need to account for 2D inhomogeneity in their concentration field.

Calculated variation of BrO vmr at sunset

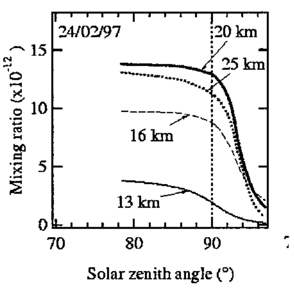

SZA variation in successive atmospheric layers (twilight)

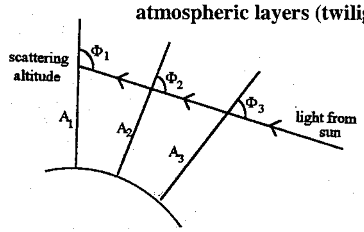

DOAS measurements from GOME

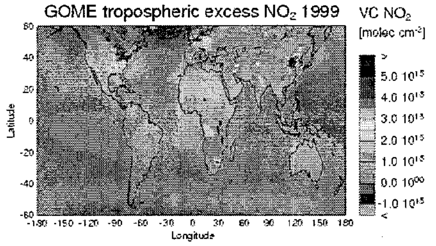

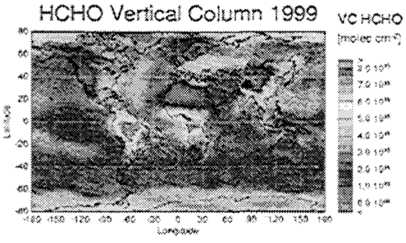

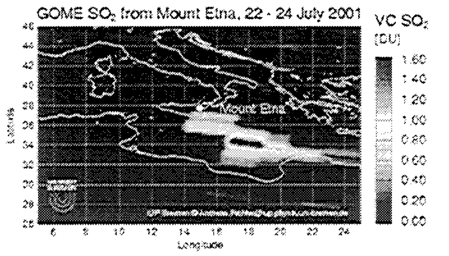

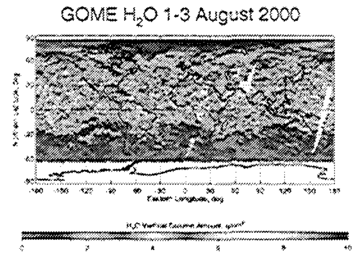

Courtesy IUP, Bremen

GOME polar spring boundary layer BrO

Monthly-averaged BrO over Arctic, April, 1996-2000

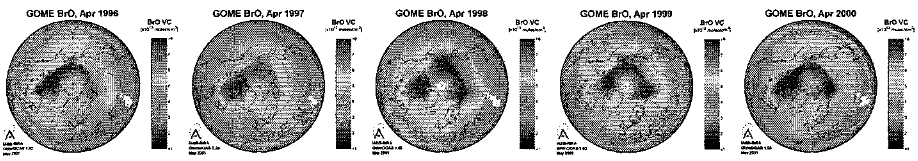

Monthly-averaged BrO over Antarctic, October, 1996-2000

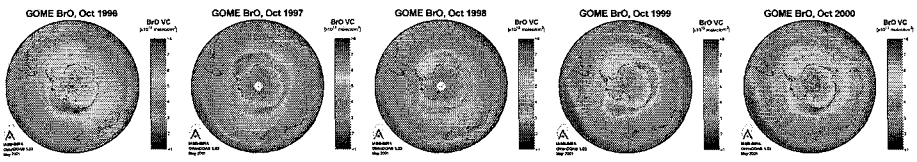

Tropospheric NO_2 from GOME

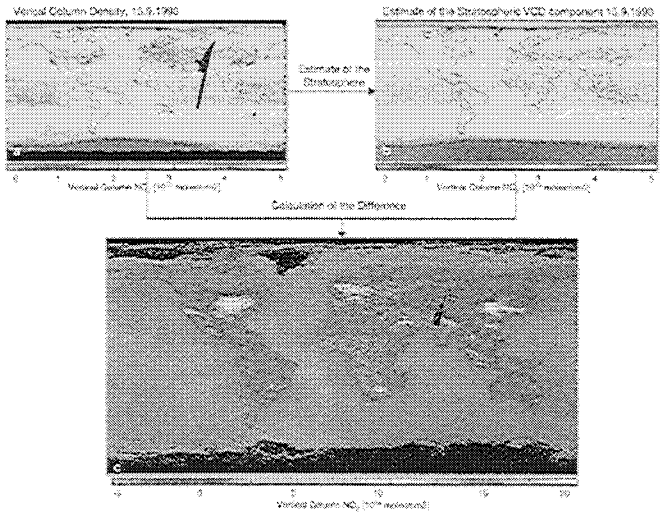

Future of DOAS

- New/extended applications
  - Long-path DOAS tomography using multiple beams
  - Multi-axis scattered light DOAS from the ground and from aircraft → probing the troposphere using passive DOAS
- Extension of DOAS towards the IR (modified DOAS aproach)
- New generation of UV-visible satellites following GOME concept (SCIAMACHY, OMI, GOME-2, ...)

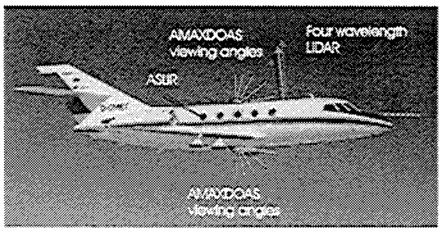

NDSC Sites

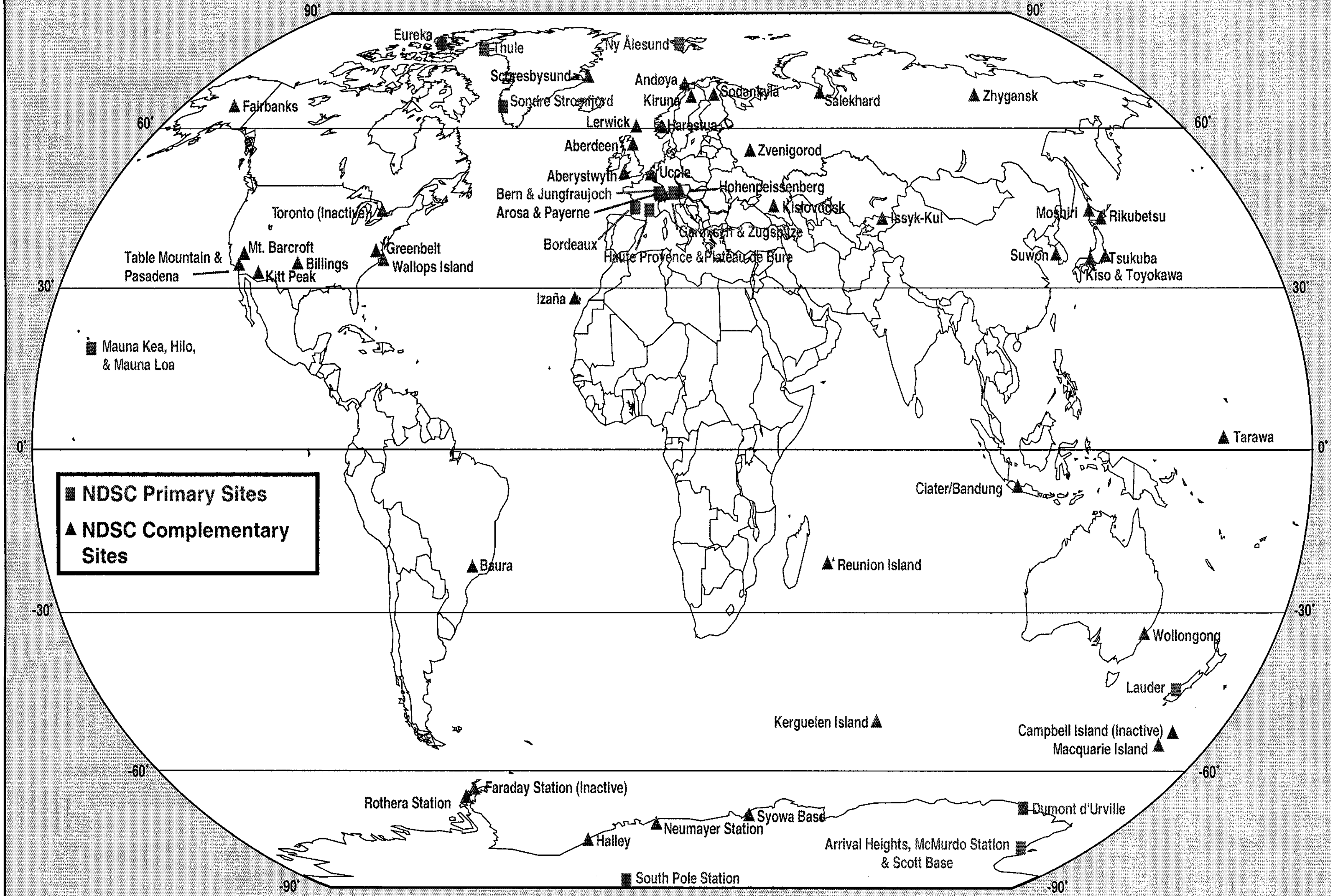

90°
60°
30°
0°
-30°
-60°
-90°
Eureka
Thule
Ny Ålesund
Scoresbysund
Sondre Stromfjord
Andøya
Kiruna
Sodankylä
Salekhard
Zhygansk
Fairbanks
Lerwick
Harestua
Aberdeen
Zvenigorod
Aberystwyth
Uccle
Bern & Jungfraujoch
Hohenpeissenberg
Arosa & Payerne
Kislovodsk
Issyk-Kul
Moshiri
Rikubetsu
Toronto (Inactive)
Garmisch & Zugspitze
Bordeaux
Haute Provence & Plateau de Bure
Suwon
Tsukuba
Kiso & Toyokawa
Table Mountain & Pasadena
Mt. Barcroft
Billings
Kitt Peak
Greenbelt
Wallops Island
Izaña
Mauna Kea, Hilo, & Mauna Loa
Tarawa
Ciater/Bandung
NDSC Primary Sites
NDSC Complementary Sites
Baura
Reunion Island
Wollongong
Lauder
Kerguelen Island
Campbell Island (Inactive)
Macquarie Island
Faraday Station (Inactive)
Rothera Station
Syowa Base
Dumont d'Urville
Neumayer Station
Halley
Arrival Heights, McMurdo Station & Scott Base
South Pole Station